Hot Corrosion of Materials: Fundamental Studies

Robert A. Rapp and Y.S. Zhang

Hot corrosion is the accelerated oxidation of materials at elevated temperatures induced by a thin film of fused salt deposit. Because of its high thermodynamic stability in the mutual presence of sodium and sulfur impurities in an oxidizing gas, Na_2SO_4 is often found to be the dominant salt in the deposit. The corrosive oxyanion-fused salts are usually ionically conducting electrolytes that exhibit an acid/base chemistry, so that hot corrosion must occur by an electrochemical mechanism that may involve fluxing of the protective oxides. With the aid of high-temperature reference electrodes to quantify an acid/base scale, the solubilities for various metal oxides in fused Na_2SO_4 have been measured, and these show remarkable agreement with the theoretical expectations from the thermodynamic phase stability diagrams for the relevant Na-Metal-S-O systems. The solubilities of several oxides in fused Na_2SO_4-$NaVO_3$ salt solutions have also been measured and modeled. Such information is important both in evaluating the corrosion resistance of materials and in interpreting any oxide fluxing/reprecipitation mechanisms. Various electrochemical measurements have identified the $S_2O_7^{2-}$ anion (dissolved SO_3) as the oxidant that is reduced in the hot corrosion process. Electrochemical polarization studies have elucidated the corrosion reactions and clarified the corrosion kinetics of alloys. Mechanistic models for Type I and Type II hot corrosion are discussed briefly.

INTRODUCTION

Metals and alloys sometimes experience accelerated oxidation when their surfaces are covered with a thin film of fused salt in an oxidizing gas atmosphere at elevated temperatures. This mode of attack is called hot corrosion. Hot corrosion first became known to engineers and researchers with the failure of boiler tubes,[1] and later with the severe attack of gas turbine airfoil materials.[2,3] In hot corrosion, metals and alloys are subject to degradation at much higher rates than in gaseous oxidation, with a porous, nonprotective oxide scale formed at their surface, and sulfides in the substrate. Hot corrosion is a serious problem in power generation equipment, in gas turbines for ships and aircraft, and in other energy conversion and chemical process systems.

Because of its high thermodynamic stability, Na_2SO_4 is found to be the common, or dominant, component of the salt deposit. Sulfur is a principal impurity in fossil fuels, and sodium is introduced into the combustion air—usually in an aerosol originating from seawater. Some other alkali or alkaline-earth sulfates may also exist in the deposit, depending upon the impurities contained in the fuel and in the intake air. Thus, thin liquid sulfate films may be deposited onto hot hardware either from the condensation of combustion products of fossil fuels,[4] or else from the direct impingement of liquid droplets from the hot gas stream. During the combustion of certain low-grade fossil fuels, vanadium compounds such as $NaVO_3$ and V_2O_5 may also be deposited in the salt film. The thermodynamics of this deposition process were analyzed by Luthra and Spacil.[5] Such corrosive oxyanion-fused salts exhibit an acid/base chemistry, with Na_2O the basic component and SO_3 the acidic component for pure Na_2SO_4. Such salts are usually also ionically conducting electrolytes. Therefore, hot corrosion must be electrochemical in nature, and may involve fluxing of the protective metal oxides as either acidic or basic solutes in the fused salt. In some aspects, hot corrosion is similar to the atmospheric corrosion of metals by thin aqueous films at ambient temperature. But the details of the mechanism with respect to the electroactive oxidant species and oxide dissolution, etc., are different.

The first technical publication on hot corrosion was contributed by Simons et al.,[6] who outlined a reaction mechanism involving metal sulfidation by Na_2SO_4, with emphasis on the accelerated oxidation of a sulfide-base eutectic. Seybolt[7] modified this sulfidation mechanism and attributed the Na_2SO_4-induced hot corrosion of Ni-Cr alloys to the accelerated oxidation of the Cr-depleted alloy following the preferential internal sulfidation of Cr. By this mechanism, sulfide formation was considered as a prerequisite for the occurrence of accelerated oxidation, and the phenomenon was even called sulfidation.

As we know today, sulfidation is not necessarily the critical mechanistic step in what is now known as "hot corrosion." Bornstein and DeCrescente[8,9] reported that accelerated kinetics were not observed during the oxidation of three different presulfidized superalloys. However, an Na_2CO_3 or $NaNO_3$ coating gave rise to accelerated kinetics similar to Na_2SO_4 in spite of the absence of sulfur in the salt. From this evidence, they proposed a hot corrosion mechanism based on the (basic) dissolution of the protective oxide scale by a reaction involving Na_2O, the basic minority component of the fused salt. During nominally the same time period, Goebel and Pettit[10] also interpreted the hot corrosion of pure Ni in terms of a basic dissolution and reprecipitation of NiO in the fused salt film. Goebel et al.[11] extended the mechanism to include acidic fluxing and oxide reprecipitation to account for the catastrophic oxidation caused by Na_2SO_4 for alloys containing strong acid components such as V or Mo. These fluxing mechanisms are still accepted today, and some quantitative aspects of oxide solubilities and electrochemical reaction steps have been added in the literature.

The phenomenology and mechanisms of hot corrosion have been extensively studied, and critically reviewed by

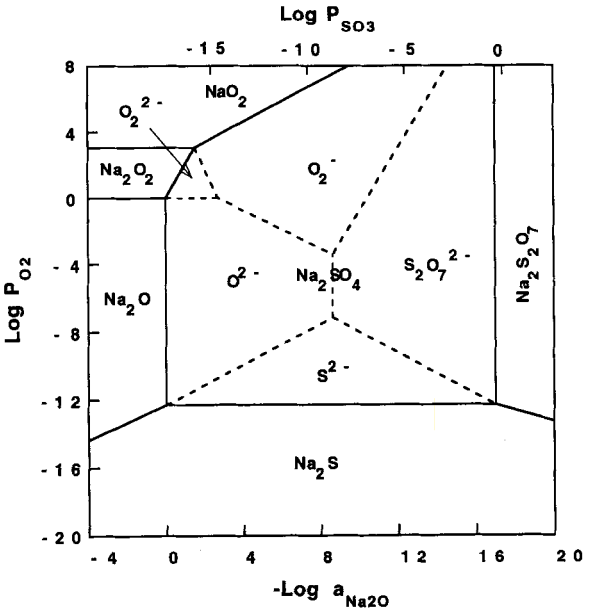

Figure 1. The Na-S-O phase stability diagram for 1,173 K.[17]

Stringer,[12,13] Pettit and Giggins,[14] and Rapp.[15,16] Some fundamental studies relating to hot corrosion mechanism are selectively presented in this article.

SALT CHEMISTRY AND PHASE STABILITY

As Na_2SO_4 is often the dominant corrosive salt in the deposit, particular attention has been paid to its chemistry and phase stability. A Pourbaix-type phase stability diagram for the Na-S-O system at 1,173 K is shown in Figure 1.[17] This diagram was constructed using the available standard Gibbs energies of formation for the relevant components and with the assumption of unit activities for the condensed phases in mutual equilibrium.

In Figure 1, liquid Na_2SO_4 is stable over a wide range of the two environmental parameters log P_{O_2} and $-\log a_{Na_2O}$ (or log P_{SO_3}). The dotted lines superimposed on the field of Na_2SO_4 stability indicate the regimes of dominance for the minority solute species under the assumption of unit activity coefficients for these solutes.

These approximate boundaries are useful in the interpretation of corrosion reactions and electrochemical studies involving the reduction of minority solutes in pure Na_2SO_4.

As described by Inman and Wrench,[18] oxyanion melts of alkali nitrates, carbonates, hydroxides, and sulfates exhibit an acid/base character whereby the acidic components may be considered as $NO_2(g)$, $CO_2(g)$, $H_2O(g)$, and $SO_3(g)$, respectively. The alkaline oxide component can be self-consistently chosen as the Lewis base in common.

For a melt of pure Na_2SO_4 (melting point 1,157 K), there exists the equilibrium

$$Na_2SO_4 = Na_2O + SO_3 \qquad (1)$$

with

$$\log a_{Na_2O} + \log P_{SO_3} = \frac{\Delta G°(1)}{2.303RT} = -16.7 \text{ (at 1,200 K)} \qquad (2)$$

The parameter $-\log a_{Na_2O}$ can be defined as the melt basicity, and $\log P_{SO_3}$ is referred to as the melt acidity. These parameters and the oxygen activity are most important in understanding oxide fluxing and electrochemical reactions. Fortunately, the values of melt basicity and oxygen activity can be measured by the use of high-temperature electrochemical reference electrodes (REs).

ELECTROCHEMICAL REFERENCE ELECTRODES

A stabilized zirconia tube with porous Pt paste painted inside the closed-end bottom serves as an oxygen probe to measure the oxygen activity at a Pt working electrode (WE) contacting the melt. The cell arrangement is

(–) Pt, O_2 (air) (RE) | (Na^+)

| Na_2SO_4, SO_3, SO_2, O_2, Pt (WE) (+) [I]

For a melt in internal equilibrium, that is, without any concentration gradient in the melt, the overall cell reaction is

$$\frac{1}{2}O_2(WE) = \frac{1}{2}O_2(RE) \qquad (3)$$

The Nernst equation for Reaction 3 describing Cell I is

$$E[I] = -\frac{RT}{4F}\ln\frac{P_{O_2}(air)}{P_{O_2}(WE)} \qquad (4)$$

with

$$E[I] = 0.0394 + 0.0582 \log P_{O_2}(WE) \text{ at 1,173 K} \qquad (5)$$

A second RE, called a sodium sensor, consists of a piece of silver wire contacting a $0.1Ag_2SO_4$-$0.9Na_2SO_4$ melt contained in a closed-end tubular Na^+-conducting electrolyte. The cell configuration is

(–) Ag, $0.1Ag_2SO_4$-$0.9Na_2SO_4$(RE)

| (Na^+) | Na_2SO_4, SO_3, SO_2, O_2, Pt (WE) (+) [II]

Either mullite or silica tubes can be used as the Na^+-conducting electrolyte, but fused silica has shown a better stability in an acidic Na_2SO_4 melt and in acidic Na_2SO_4-$NaVO_3$ salt solutions. Since both the electrolyte and the sodium melt provide exclusive Na^+ conduction, the cell equation involves the ratio of the thermodynamic activities of sodium at the RE and the WE:

$$E[II] = -\frac{RT}{F}\ln\frac{a_{Na}(RE)}{a_{Na}(WE)} \qquad (6)$$

Shores and John[19] evaluated a_{Na}(RE) for 1,173 K to give

$$E[II] = -1.472 - 0.116 \log\frac{a_{NaO}(WE)}{P_{O_2}(WE)} \qquad (7)$$

The melt basicity can be determined by combining the voltages of cell [I] and cell [II]:

$$E = E[II] - E[I] = -1.466 - 0.116 \log a_{Na_2O} \text{ (WE) at 1,173 K} \qquad (8)$$

These two reference electrodes have been used successfully for a pure Na_2SO_4 melt and for other Na^+-cation salt solutions such as Na_2SO_4-$NaVO_3$, Na_2SO_4-Na_2CrO_4, etc.

However, for solutions with a common anion but multiple cations, such as a Na_2SO_4-K_2SO_4-$Fe_2(SO_4)_3$ ternary melt, the sodium sensor is no longer valid. For this ternary sulfate solution, Leblanc and Rapp[20] developed another reference electrode comprised of a fused silica tube with a small hole at the bottom. Excess hematite (α-Fe_2O_3) powder was held within the tube. The hole allowed some of the ternary sulfate melt to enter the tube and be saturated with Fe_2O_3, thereby fixing its activity for SO_3. However, at the Pt WE outside the tube, the salt melt whose acidity was to be measured was not saturated with Fe_2O_3. The cell arrangement is

(–) Pt (RE), Fe_2O_3, melt | melt | melt, SO_3, Pt (WE) (+) [III]

The following equilibrium is maintained for the common melt composition at both the RE and WE,

$$SO_3 + \frac{1}{2}O_2 + 2e^- = SO_4^{2-} \qquad (9)$$

Then E[III] is interpreted as

$$E[III] = -\frac{RT}{2F}\ln\frac{P_{SO_3}(RE)}{P_{SO_3}(WE)} - \frac{RT}{4F}\ln\frac{P_{O_2}(RE)}{P_{O_2}(WE)} \qquad (10)$$

In this way, P_{SO_3} in the working melt can be measured if the oxygen activity ratio is fixed and known. Thus, this cell provides a measurement of melt acidity, defined as log P_{SO_3}. This reference electrode was used for measurements of the solubilities of Cr_2O_3 and SiO_2 in a $0.71Na_2SO_4$-$0.18K_2SO_4$-$0.11Fe_2(SO_4)_3$ ternary sulfate solution at 963 K.[21]

OXIDE SOLUBILITIES

Upon contacting a fused salt, metals and alloy components are oxidized to form thin oxide scales whose protectiveness depends upon the stability

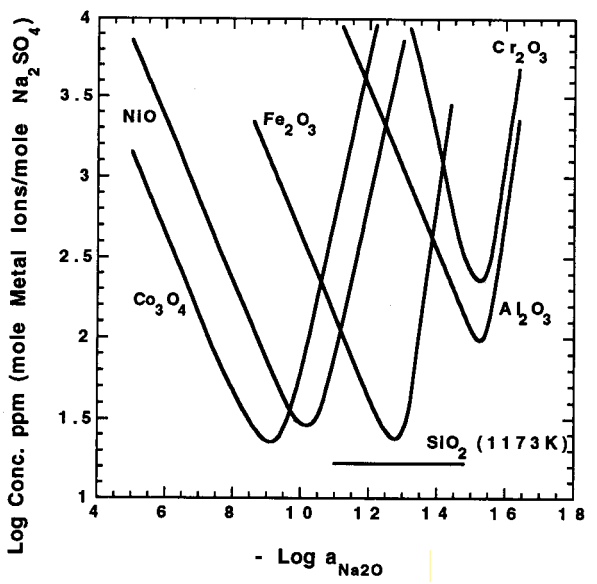

Figure 2. Measured oxide solubilities in fused Na_2SO_4 at 1,200 K and 1 atm. O_2.[15]

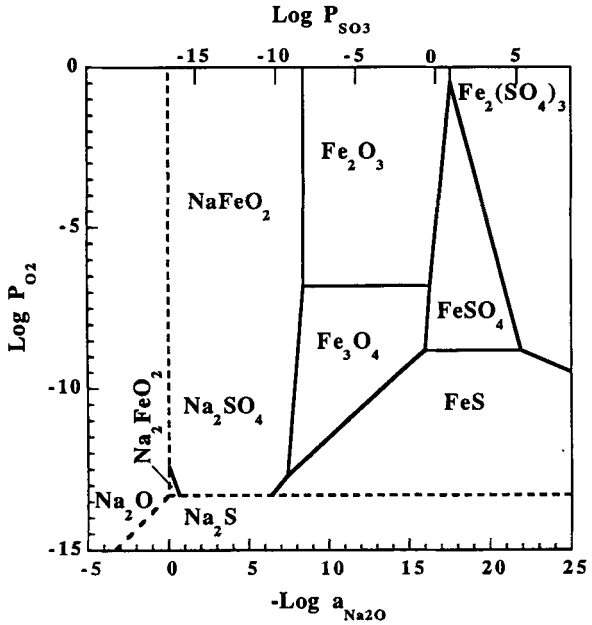

Figure 3. The Na-Fe-S-O phase stability diagram for 1,200 K.[23]

of the oxide in the salt. For this reason, a knowledge of oxide solubilities in the fused salt is important in evaluating the hot corrosion resistance of materials.

Pure Na_2SO_4 Melt

From a knowledge of the Na-Metal-S-O phase stability diagrams, and by the use of the high temperature reference electrodes of cells [I] and [III] to indicate the activities of sodium oxide and oxygen, the solubilities of the oxides NiO and Co_3O_4,[22] Fe_2O_3 and Fe_3O_4,[23] Cr_2O_3,[24] Al_2O_3,[25] and SiO_2[26] in pure fused Na_2SO_4 have been measured as a function of melt basicity at 1200 K and 1 atm oxygen, as summarized in Figure 2. The solubilities of NiO and Co_3O_4 in pure Na_2SO_4 were also measured by Deanhardt and Stern,[27] and by Misra, Whittle and Worrell.[28] The measurements of these studies are self-consistent. Deanhardt and Stern[29] also established experimentally the solubility of Y_2O_3 as a function of Na_2SO_4 basicity. Except for SiO_2, all the oxides dissolve in the melt as either basic or acidic solutes, depending upon melt basicity. From the dependence of oxide solubilities on melt basicity, in combination with the Na-Metal-S-O phase stability diagrams, the solute species were identified and their activity coefficients were derived for the dilute solutions. In Figure 2, the six orders of magnitude difference in -log a_{Na_2O} values for the solubility minima between the basic oxides Co_3O_4 or NiO and the acid oxides Al_2O_3 or Cr_2O_3 emphasize the importance of the local chemistry in a fused salt film.

Certain phase stability diagrams, as shown for example in Figure 3 for the Na-Fe-S-O system, indicate that the solubilities of oxides such as the iron oxides (and Cr_2O_3) with multi-valent solutes should depend not only on melt basicity but also on oxygen activity. Figure 4 shows the solubilities of Fe_2O_3 and Fe_3O_4 in fused Na_2SO_4 at 1,200 K for the four solutes $Fe(SO_4)_{1.5}$, $FeSO_4$, FeS, and $NaFeO_2$.[23] The solid curves in Figure 4 describe the measured solubility values at certain oxygen activities, and the dashed lines are calculated for some other oxygen pressures. A similar solubility "map" for Cr_2O_3 was also established.[24] These detailed experimental results show excellent agreement with theoretical expectations, and provide values for the activity coefficients for the solutes in the dilute solutions. Such data are useful in interpreting any oxide fluxing/reprecipitation mechanisms in a thin salt film with gradients in oxygen and sodium oxide activities.

According to Figure 2, silica exhibits a solubility behavior different from the other oxides, namely, in reasonably acidic melts, the solubility of silica does not depend upon melt basicity. This means that silica forms only a molecular, nonionized solute of low concentration. However, in more basic melts, silica does form a basic solute. The lack of an acidic solute for silica means that it is not subject to dissolution/reprecipitation hot corrosion attack in acidic melts, as explained later. Recent papers by Jacobson et al.[30,31] are consistent with these solubility considerations. They also point out the advantage of high-sulfur fuels in stabilizing silica protective scales.

According to the widely spaced solubility curves of Figure 2, one would suggest that the simultaneous contact with fused Na_2SO_4 of two oxides with solubility minima at different basicity values could result in a synergistic accelerated dissolution of both oxides. Specifically, for a salt environment with a basicity value lying between the minima for any two oxides in Figure 2, the oxide ions released upon the acidic dissolution of the more basic oxide would supply the reactant anions needed for the basic dissolution of the more acidic oxide, e.g. for the coupled dissolution of Fe_2O_3 and Cr_2O_3:

$$\frac{2}{3}Fe_2O_3 \rightarrow \frac{4}{3}Fe^{3+} + 2O^{2-} \quad (11)$$

(acidic dissolution)

$$Cr_2O_3 + 2O^{2-} + \frac{3}{2}O_2 \rightarrow 2CrO_4^{2-} \quad (12)$$

(basic dissolution)

$$\frac{2}{3}Fe_2O_3 + Cr_2O_3 + \frac{3}{2}O_2 \rightarrow 2CrO_4^{2-} + \frac{4}{3}Fe^{3+} \quad (13)$$

(coupled dissolution)

Hwang and Rapp[32] measured the rates for the individual and the coupled dissolution for Fe_2O_3 and Cr_2O_3 powders in fused Na_2SO_4 at 1,200 K for log $a_{Na_2O} = -14.0$. As illustrated in Figure 5, in accordance with the prediction of Equation 13, each of the oxides dissolved much more rapidly in the presence of the other oxide for identical conditions otherwise. Synergistic dissolution represents a potential problem for high-temperature engineering alloys forming a basic oxide from the base metals Fe, Ni, or Co in combination with an acidic oxide formed from the protective elements Cr or Al. The practical avoidance of synergistic dissolution attack in the usual acidic melts for alloys such as stainless steels or superalloys is to ensure that the alloy or coating composition forms a protective scale of Cr_2O_3 or Al_2O_3 with the exclusion of Fe_2O_3, NiO, or CoO.

Na_2SO_4-$NaVO_3$ Salt Solutions

As mentioned above, the use of certain low-grade fuels leads to the condensation of vanadium compounds in addition to sulfates,[5] and these fused-salt solutions are extremely corrosive to

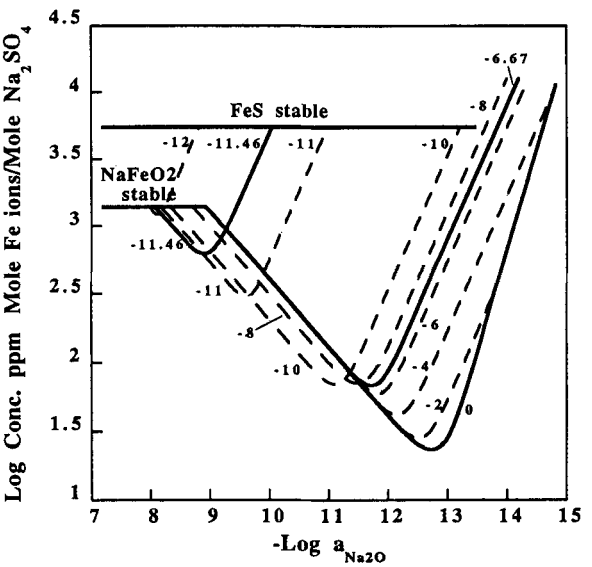

Figure 4. Measured (solid lines) and calculated (dashed lines) solubilities of Fe_2O_3 and Fe_3O_4 in fused Na_2SO_4 at 1,200 K for several oxygen activities. Numbers in the figure designate the partial pressures of oxygen.[23]

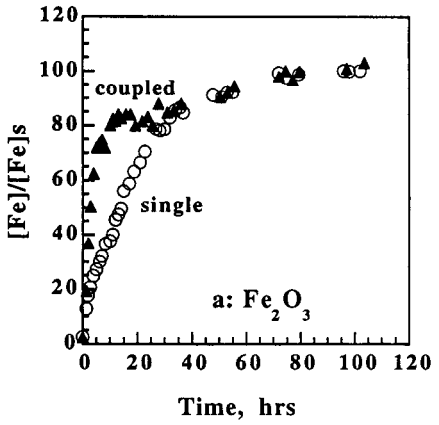

a

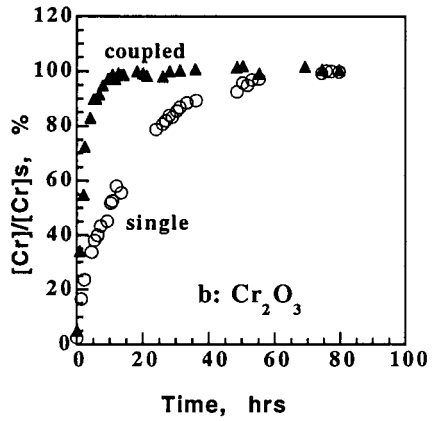

b

Figure 5. Time dependence of the normalized concentrations of (a) dissolved Fe_2O_3 and (b) Cr_2O_3 in fused Na_2SO_4 in O_2-1%SO_2 gas at 1,200 K.[32]

high-temperature materials. To provide direction in the selection of oxide-thermal barrier-coating components that are resistant to sulfate-vanadate melts, the solubilities of the oxides CeO_2, HfO_2, and Y_2O_3 in a $0.7Na_2SO_4$-$0.3NaVO_3$ solvent melt were measured as a function of melt basicity at 1,173 K, as illustrated in Figure 6.[33] For comparison, the solubility of CeO_2 in a pure Na_2SO_4 melt was also determined. Metal orthovanadates were shown to be the dominant acidic solutes, with much higher acidic solubilities in a vanadate melt than in pure Na_2SO_4 at the same solvent basicity. The existence of much higher acidic solubilities in a sulfate-vanadate melt compared to pure Na_2SO_4 is decided by the complexing of oxide ions by the metavanadate to form orthovanadate ions, so that this deleterious effect is generally expected for all oxides.

Hwang and Rapp[34] assumed an ideal solution for the $0.7Na_2SO_4$-$0.3NaVO_3$ system and calculated the equilibrium concentrations of the vanadium compounds at 1,173 K as a function of Na_2O activity, as shown in Figure 7. This analysis (on the ideal solution assumption) was confirmed recently[35] by measuring the Na_2O activities for Na-V-S-O melts with ratios of Na:V from 1:9 to 9:1 at 1,173 K and a fixed $P_{SO_3} = 10^{-2.66}$ atm. The measured values compared well with those theoretically calculated on the basis of an ideal sulfate/vanadate solution. The assumption of an ideal solution for Na_2SO_4-$NaVO_3$-V_2O_5 melts[34] permits quite general predictions for the dependence of oxide solubilities on salt composition. As presented in Figure 8, the experimentally measured solubility for CeO_2 in the $0.7Na_2SO_4$-$0.3NaVO_3$ melt has served as the basis for the calculation of CeO_2 solubility with lower vanadate content. The experimental points for the $0.9Na_2SO_4$-$0.1NaVO_3$ melt show new measurements that agree well with the prediction based on an ideal solution for the sulfate/vanadate solvent. Even a small vanadate content in such salt solutions causes a significant increase in the acidic solubility for any oxide. Again, this general behavior results because of the complexing of oxide ions by the vanadate component regardless of the oxide suffering dissolution.

On the subject of hot corrosion induced by vanadium compounds, much work has been done. For example, Jones et al.[36-40] studied the chemical stabilities of various oxides, such as Y_2O_3, CeO_2, HfO_2, In_2O_3, Sc_2O_3, and ZrO_2 in V_2O_5, $NaVO_3$, or Na_2SO_4 fused salt solutions. Seiersten and Kofstad[41] studied the hot corrosion of MCrAlY coatings on Inconel 600 alloy by fused $NaVO_3$-V_2O_5 solutions and found that the corrosion rate increased with increasing V_2O_5 content. Nagelberg[42] reported that the parabolic rate constant for the leaching of Y_2O_3 from Y_2O_3-stabilized ZrO_2 in Na_2SO_4-$NaVO_3$ melts at 1,173 K was proportional to the SO_3 partial pressure and the square of $NaVO_3$ concentration. These results are consistent with the oxide solubility measurements described above.

ELECTROCHEMISTRY OF HOT CORROSION

Electrochemical (EC) measurements have been performed to establish the important kinetic steps in the hot corrosion mechanism.

EC Reduction Reaction

The geometric similarity of hot corrosion of metals by a thin salt film at high temperatures to that for the atmospheric corrosion of metals at ambient temperature by a thin aqueous film implies some common mechanistic characteristics and rate-limiting step. As demonstrated by Mansfeld and Kenkel,[43,44] aqueous atmospheric corrosion is limited by the diffusion of molecular oxygen across the water film. However, the volumetric measurements of Andresen[45] revealed relatively low solubilities for O_2 and SO_2 in the Na_2SO_4 melt. Shores and Fang[46] measured the limiting cathodic current densities for very thin fused Na_2SO_4 films on Pt exposed to various $O_2/SO_2/SO_3$ gas environments, and demonstrated that SO_3 (as $S_2O_7^{2-}$) was the oxidant that diffused and supported electrochemical reduction, with only a small contribution by diffusion of dissolved O_2. Fang and Rapp[47] performed cyclic voltammetry and chronopotentiometry measurements using a three-electrode arrangement in Na_2SO_4 with $O_2/SO_2/SO_3$ in the gas phase and proposed the following reduction reaction sequence:

$$SO_3 + SO_4^{2-} \leftrightarrow S_2O_7^{2-} \quad (14)$$

(chemical equilibrium)

$$S_2O_7^{2-} + e^- \rightarrow SO_4^{2-} + SO_3^- \quad (15)$$

followed by the gain of a second electron

$$SO_3^- + e^- \rightarrow SO_2 + O^{2-} \quad (16)$$

In the cathodic polarization of nickel, Numata et al.[48] observed an increase in the diffusion-limiting current with the addition of pyrosulfate to the electrolyte. Again, the electrochemical reduction step in an acidic sulfate melt was inferred to be the reduction of SO_3.

Park and Rapp[17] have clarified the EC reactions using a three-electrode polarization experiment, at least for a nominally nonreactive Pt WE in pure Na_2SO_4 with an $O_2/SO_2/SO_3$ environment at 1,173 K. In combination with Figure 1, the measured trace of local melt chemistry resulting from cathodic polarization from the open-circuit potential showed that the pyrosulfate ion was reduced. As shown in Figure 9, initially, the cathodic reduction of the $S_2O_7^{2-}$ solute resulted in a small increase in melt basicity with a

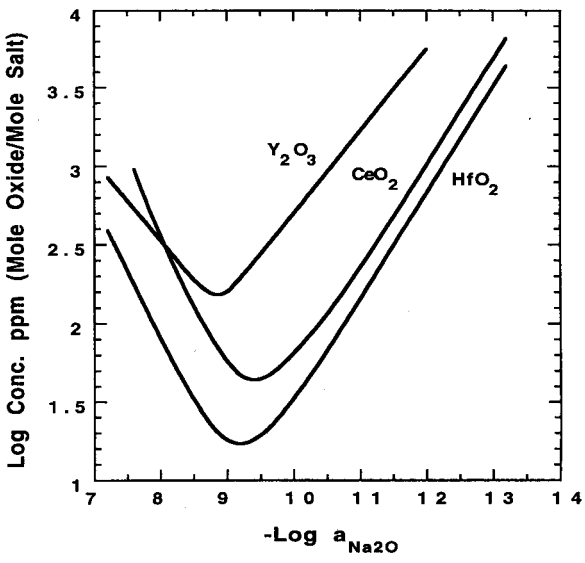

Figure 6. Measured solubilities of CeO_2, HfO_2 and Y_2O_3 in $0.7Na_2SO_4$-$0.3NaVO_3$ at 1,173 K and 1 atm O_2.[33]

small decrease in the oxidizing potential. Upon depletion of the pyrosulfate oxidant and in the absence of another, further cathodic polarization caused a sharp drop in oxidation potential at virtually constant basicity as the very low dissolved oxygen content was consumed. Finally, at a very reducing potential where Na_2S was stabilized, the melt shifted in a basic direction as the sulfate ion was reduced. Such an EC experiment with Pt should not be considered as irrelevant to the hot corrosion of an engineering alloy, because if a protective oxide scale is penetrated by the salt film to contact the metal, the effect on local salt chemistry is equivalent to a deep cathodic polarization, which could result in metal sulfidation.

Zheng and Rapp[49] used EC impedance spectroscopy to study the reduction reaction at a Pt electrode in a pure Na_2SO_4 melt with an $O_2/SO_2/SO_3$ gas atmosphere. The $S_2O_7^{2-}$ ion was again found to be the dominant oxidant for the reduction reaction in the melt regime where the minority solute $S_2O_7^{2-}$ was dominant. A relatively large Warburg impedance was observed at low frequency, which indicated a rate-limiting diffusion step. All these studies have identified $S_2O_7^{2-}$ as the oxidizing agent that is reduced in hot corrosion attack provided a certain content of SO_3 is present in the corrosion environment.

In the absence of SO_3, and upon doping Na_2SO_4 with 5 mol.% Na_2O_2, cyclic voltammetry and chronopotentiometry studies[47] of a Pt electrode revealed that a chemical equilibrium step

$$O_2^{2-} + O_2 = 2O_2^- \qquad (17)$$

was followed by a reduction reaction involving three or four electrons according to

$$O_2^- + 3e^- \rightarrow 2O^{2-} \qquad (18)$$

or

$$2O_2^- + 4e^- \rightarrow 2O^{2-} + O_2^{2-} \qquad (19)$$

According to the regimes of solute dominance indicated in Figure 1, these reactions are reasonable for basic melts.

In the presence of higher valent cations of transition metals in sulfate melts, these cations could be expected to be involved in the EC reduction reaction. Numata and Haruyama[50] studied the EC polarization of iron in a deep $(Na,K,Li)_2SO_4$ melt containing $Fe_2(SO_4)_3$ with a $1\%SO_2$–$5\%O_2$–$94\%N_2$ gas at 973 K, and demonstrated the anodic dissolution of iron and the cathodic reduction of ferric ions in the potential region from 0.3 to –0.5 V (Ag/Ag^+). The polarization study demonstrated that the corrosion of iron would be controlled by the diffusion-limited cathodic reduction of ferric ions, which would be proportional to the ferric ion concentration.

Transient EC studies have also been performed to clarify the role of the anionic solutes of strong acids on the electrochemical reduction step. Kupper and Rapp[51] reported cyclic voltammetric measurements as a function of melt basicity for molybdate ions in fused Na_2SO_4 at a Pt electrode at 1,200 K. The reduction of MoO_4^{2-} in a highly acidic melt resulted in the precipitation of solid MoO_2. In less acidic melts, MoO_4^{2-} ions were reduced reversibly to MoO_3^{2-} without MoO_2 precipitation. In the most basic melts, the electron transfer from the +5 oxidation state to +4 was inhibited and became rate limiting. The polarization traces plotted onto the Na-Mo-S-O phase stability diagram supported the proposed mechanism. The authors also demonstrated a buffering behavior for these melts.

Nava et al.[52] conducted extensive transient EC studies at a Pt WE at 1,173 K for Na_2SO_4-$NaVO_3$ solutions and obtained similar results. For a given melt basicity, both cyclic voltammetry and chronopotentiometry indicated that a reversible one-electron reduction reaction was followed by an irreversible chemical reaction. Because of the buffering action by VO_3^-/VO_4^{3-} ions, a negligible shift in melt basicity resulted from the redox reactions. In an acidic sulfate melt containing V_2O_5 and $NaVO_3$, the reduction "path" passed through a field of solid VO_2 on the stability diagram, so that an irreversible precipitation of solid VO_2 caused a shift to high melt basicity in the solution.

Shi and Rapp[53] reported transient EC studies at a Pt WE at 1,200 K for Na_2SO_4/Na_2CrO_4 solutions. In quite acidic solutions, Cr_2O_3 precipitated chemically so that no important EC chromate reduction reactions could be observed. For neutral and basic solutions, the chromate ion was not an electroactive solute. Only one cathodic reaction was detected: a reversible charge transfer process involving one electron. The electroactive species was deduced to be CrO_4^{3-}, which was formed by a chemical equilibrium between CrO_4^{2-} and O^{2-} ions in the solution. An irreversible chemical reaction followed the cathodic process, and the resulting reaction product was Cr_2O_3 in the neutral melt, and solid $NaCrO_2$ in the basic melt. The protective nature of Cr as an alloy component and of a Cr_2O_3 scale may be explained, in part, by the healing precipitation of Cr_2O_3 or $NaCrO_2$ into cracks or crevices of the protective scale.

Corrosion Kinetics Studies for Alloys

Using a three-electrode arrangement, several researchers have studied the anodic and cathodic polarization behavior of engineering alloys in "deep" sulfate melts. Shores[54] investigated the anodic polarization behavior of preconditioned Ni-and Co-base superalloys in Na_2SO_4 at 1,179 K using a Pt/O_2-ZrO_2 RE, and demonstrated that the corrosion currents

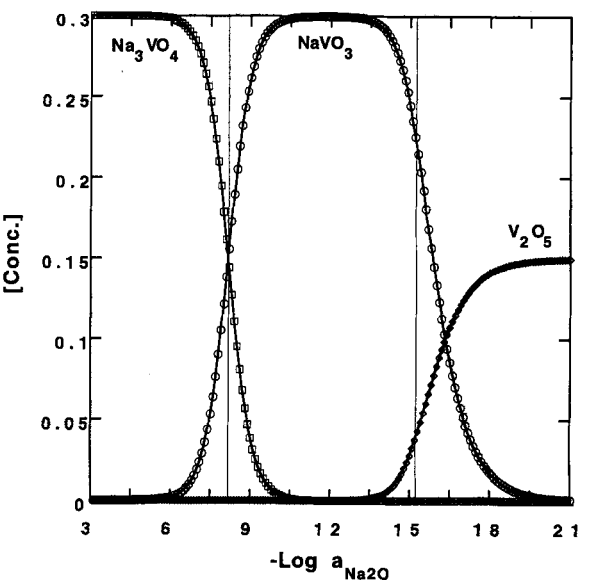

Figure 7. Equilibrium concentrations of Na_3VO_4, $NaVO_3$ and V_2O_5 in sodium sulfate-vanadate solution containing 30 mol.% vanadium at 1,173 K.[34]

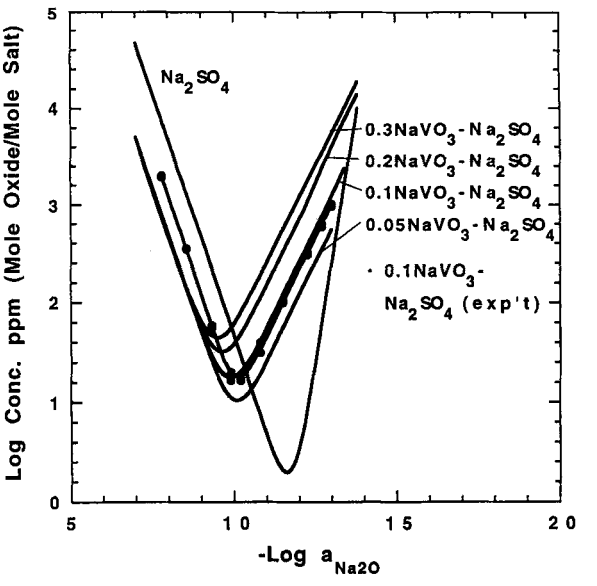

Figure 8. Solubilities of CeO_2 in pure Na_2SO_4 and Na_2SO_4-$NaVO_3$ solutions at 1,173 K and 1 atm O_2.[35]

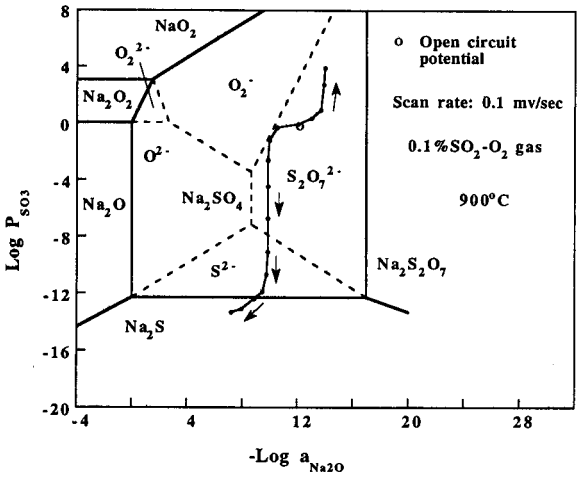

Figure 9. Trace of basicity and oxygen activity measured on a porous Pt working electrode.[17]

determined from the extrapolation of Tafel slopes correlated with the corrosion attack of alloys observed in burner rig tests. Measurements of anodic polarization, polarization resistance, and corrosion potential using a Ag/Ag^+ RE were conducted by Numata et al.[48] to interpret the hot corrosion behavior of nickel and its alloys in a "deep" binary Na_2SO_4-Li_2SO_4 melt at 973 K. The relatively high anodic currents were attributed to metal dissolution through an oxide film on the metal surface. The polarization resistance measurements correlated well with the measured corrosion rates.

Rahmel et al.[55] conducted polarization studies in deep melts to evaluate the hot corrosion behavior of nickel- and cobalt-base superalloys in a ternary $0.53Na_2SO_4$-$0.4MgSO_4$-$0.07CaSO_4$ melt and in a binary $0.9Na_2SO_4$-$0.1K_2SO_4$ melt with a pure oxygen atmosphere at 1,173 K. For a given alloy, anodic polarization caused severe corrosion attack due to acidic fluxing. For the ternary melt containing $MgSO_4$, inhibition was found upon cathodic polarization due to MgO precipitation and incorporation into the scale. For nickel-base alloys in a binary $(Na,K)_2SO_4$ melt at 1,173 K, Wu and Rahmel[56] performed potentiostatically controlled corrosion experiments, as well as measurements of the free corrosion potentials and polarization resistances. A passive, protective scale was observed for the chromia-forming alloys at intermediate potentials. At more anodic potentials, however, the alloys underwent rapid corrosion due to acidic fluxing. Cathodic polarization at potentials below the passive region induced rapid attack by basic fluxing with the formation of internal sulfides. Alumina-forming alloys did not form a protective scale at any potential. However, aluminide-or platinum-modified aluminide coatings, which form more protective Al_2O_3 scales, showed more or less the same electrochemical corrosion behavior as the chromia-forming alloys.[57] The corrosion potential and polarization resistances obtained were consistent with the potentiostatic polarization measurements. Furthermore, on the basis of the EC measurements, the alloys or coatings could be ranked in good agreement with the results of other tests, and even with their behavior in gas turbine service.

Recently, a technique of weak polarization with a computer-aided fitting of the polarization curve was developed by J. Zhang et al.[58,59] Clearly, reactions on a corroding electrode in high-temperature molten salts are quite different from those in aqueous solutions at ambient temperature. For the latter case, only one irreversible (rate-limiting) reaction is often assumed for either the cathodic or anodic process with the neglect of competing reactions. However, for electrochemical reactions in molten salts (nearly reversible), electron exchange reactions and concurrent reactions for the cathodic and anodic processes must be considered. The polarization equations were fit with a program for finding optimum solutions, and corrosion rates for a series of alloys were calculated.

Although sometimes EC polarization in deep melts can produce corrosion behavior similar to that caused by a thin salt film in a combustion environment, the geometric difference and the resulting chemical response between laboratory tests and the real engineering problem cannot be minimized. Clearly, EC hot corrosion studies under a thin salt film are necessary for the eventual understanding of hot corrosion kinetics and for the correlation between laboratory experiments and engineering practice.

HOT CORROSION MECHANISMS

The subject of hot corrosion has been an active research area, but certainly a detailed mechanistic understanding of the attack of any alloy under any conditions is not possible yet. However, from the available literature, particularly considering the best studies, some opinionated generalizations can be offered. First, early work[8–11] revealed the critical importance of oxide fluxing, at least in the absence of an applied tensile load. Today, quantitative measurements of oxide solubilities as presented in Figures 2, 4, 6, and 8 are available, along with an improved knowledge of phase stabilities, condensation criteria, salt chemistry, and EC techniques and responses, to permit more detailed explanations.

Type I Hot Corrosion

Stringer[12] discussed the temperature dependence for the occurrence of hot corrosion and the corresponding corrosion morphologies and kinetics. High-temperature (Type I) hot corrosion (HTHC) is nominally observed in the temperature range of about 825–950°C when the condensed salt film is clearly liquid (melting point of pure Na_2SO_4 is 884°C). The typical microstructure for HTHC shows the formation of sulfides and a corresponding depletion of the reactive component in the alloy substrate. The external corrosion products frequently comprise oxide precipitates dispersed in the salt film. From the phase stability diagrams, there are hardly any local conditions under which the important metallic components can directly contact liquid Na_2SO_4 without the formation of sulfides, so a pore, crevice, or crack across a protective oxide film can certainly lead to sulfidation in the alloy substrate and a resulting significant shift in the basicity of the salt film. Once the fused salt contacts the alloy substrate to effect sulfidation, the rate and duration of the rapid corrosion kinetics should be decided by the magnitude and gradient of the salt basicity relative to the local solubilities for the oxide scale phases, as quantified by their solubility plots.[22–29]

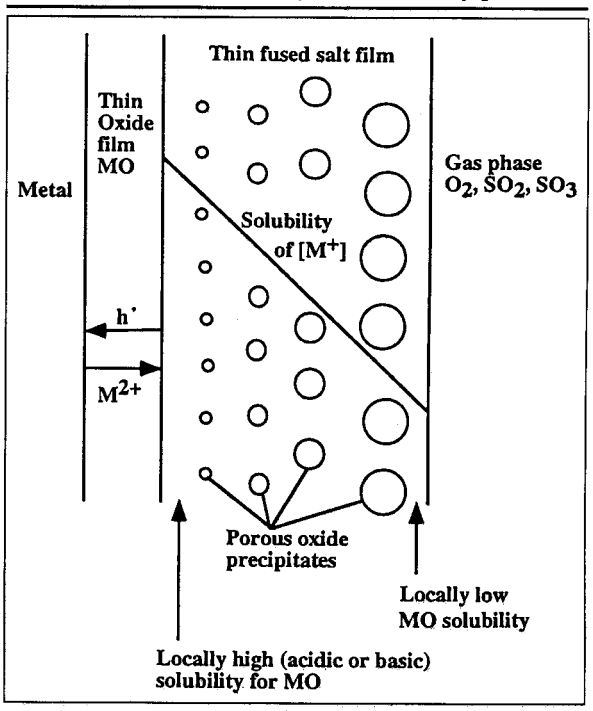

Figure 10. Reprecipitation of a porous MO oxide supported by the solubility gradient in a fused salt film.[60]

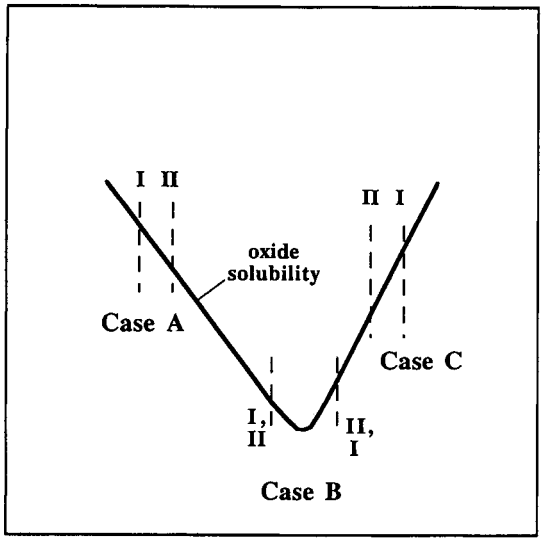

Figure 11. Cases of sustained hot corrosion of a pure metal (I is the oxide/salt interface, and II is the salt/gas interface).[60]

As a criterion for sustained hot corrosion of pure metal, Rapp and Goto[60] suggested the gradient in the solubility of the protective oxide in the salt film is negative at the scale/salt interface:

$$\left(\frac{d[\text{oxide solubility}]}{dx}\right)_{x=0} < 0 \qquad (20)$$

Then, as illustrated in Figure 10, the oxide scale would dissolve to its saturation concentration at the scale/salt interface. The solute would diffuse down a concentration gradient in the salt film and reprecipitate the oxide as nonprotective particles where the oxide solubility was locally exceeded. In terms of a schematic solubility plot for a single component, Figure 11 presents combinations of basicity gradients in the salt film that would lead to oxide reprecipitation following acidic or basic dissolution of the protective scale.[60]

Figure 11 illustrates schematically four different sets of basicities at the scale/salt interface I and salt/gas interface II superimposed on an oxide solubility plot. Those sets of conditions that would set up a negative solubility gradient in the salt film should sustain hot corrosion of a pure metal, according to the model of Figure 10 and Equation 20. The model can also be extended for application to the most reactive component of an alloy. Cases A and C of Figure 11 represent the conditions for the occurrence of persistent hot corrosion by basic and acidic fluxing, respectively. The solubility of the basic solute (case A) or the acidic solute (case C) at the scale/salt interface is greater than that at the salt/gas interface, so that a negative solubility gradient in the salt film is established. If the dominant interfacial basicities for interfaces I and II were reversed, the entire salt film should simply saturate with the oxide consistent with the basicity of interface I, and then the dissolution reaction should stop (no sustained reprecipitation). For case B, persistent hot corrosion would also be expected whenever the local basicities at interfaces I and II straddle the minimum in oxide solubility. For some oxides, the solubility depends upon both melt basicity and oxygen activity, and, therefore, the effects of both parameters on the local solubility in the film must be considered.

Rapp and Goto[60] suggested that the EC reduction reaction should generally be expected to create a condition of locally high basicity, since reduction reactions may generate oxide ions as reaction products. The oxide/salt interface is generally the site for the EC reduction reactions for oxidant species dissolved in the salt film, and therefore this interface may be the most basic location in the salt film. The oxide scale would form either acidic or basic solutes there, depending on the solubility plot. In some cases, however, the site for reduction of the oxidant species may be shifted to the salt/gas interface if the electronic charge can be carried through the salt film either by the counter diffusion of two differently charged transition metal ions, or else as electronic conduction in the film resulting from electron hopping between the transition metal species. For these cases, the most basic location in the salt film should be the salt/gas interface. Thus, the gradient in basicity across the salt film could be decided dominantly by the location of the EC reduction reaction.

Shores[61] generally analyzed Type I hot corrosion, and specifically the Rapp-Goto dissolution/precipitation criterion for the hot corrosion of pure Ni. Shores noted the importance of the salt film thickness, in combination with the gas composition, in deciding the acid-base state at the oxide/salt interface. A thick salt film in gaseous environments dilute in SO_3 cannot avoid a shift to basic conditions at the substrate as the pyrosulfate ion is reduced. Experimentation in air or oxygen is subject to this criticism. Shores[61] showed that highly corroded alloys yield dry, porous product zones, and the wet covering film of Figure 10 is more descriptive of a resistant alloy with an extremely thin oxide film. The author concluded that the hot corrosion of Ni by the acidic gaseous environment of gas turbine combustion products cannot lead to basic dissolution that would satisfy the "negative solubility gradient" criterion.

Recently, Otsuka and Rapp[62] used high-temperature probes attached to preoxidized Ni coupons, which were then exposed to a thin salt film of Na_2SO_4 in a catalyzed O_2-0.1%SO_2 gas at 1,173 K, to measure the local (average) salt chemistry, in terms of oxygen and Na_2O activities, as a function of reaction time. In one "thin film" EC experiment, after 15 minutes of exposure, the fused salt penetrated the preformed oxide scale, leading to the sulfidation of Ni. As shown in Figure 12, which plots the "reaction trace" as a function of time, a Ni coupon which suffered rapid sustained hot corrosion in an acid gas actually was attacked by a basic dissolution to form a basic solute for NiO, to the left of the NiO solubility minimum shown in Figure 12. In fact, the chemistry of the thin salt film was dominated by its contact with the substrate, where a sulfidation reaction led to a large increase in basicity, in agreement with the model of Goebel and Pettit.[11] In a different experiment, in which a preoxidized Ni coupon was exposed directly to a quite basic salt, rapid hot corrosion resulted although substrate sulfidation did not occur.[62] In other experiments, hot corrosion was avoided by the formation of more protective initial NiO scales. In that case, the local salt chemistry always remained to the right

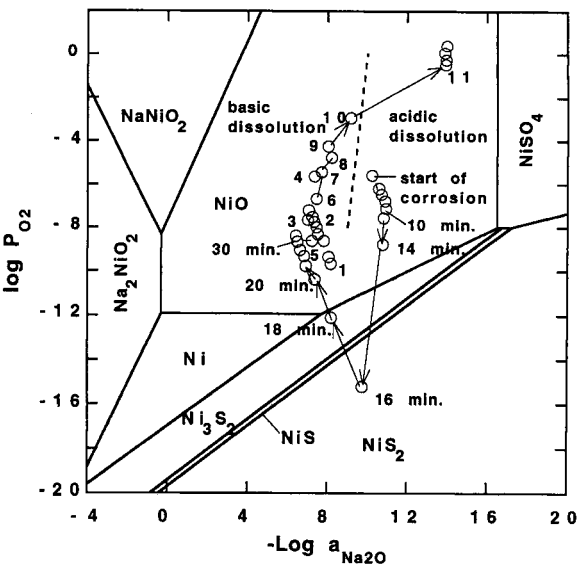

Figure 12. Trace of basicity and oxygen activity measured on a preoxidized 99% Ni coupon covered with a Na_2SO_4 film at 1173 K in O_2–0.1%SO_2 gas .[62] Numbers in the figure designate the reaction time in hours, except as indicated.

(acidic) side of the solubility minimum of Figure 12, close to an equilibrium with the acid gas. These studies clearly validated the "negative solubility gradient" criterion.

More recently, Wu and Rapp[63] made EC impedance measurements on preoxidized Ni under a thin salt film of Na_2SO_4 in a 0.1%SO_2-O_2 gas at 1,200 K, and demonstrated three distinct modes of hot corrosion: passive, pseudo-passive, and active. In the passive state, the impedance response for 99.9975% pure Ni (oxide film thickness ~4.3 μm) was attributed to an interfacial reaction impedance at the oxide/salt interface and to an impedance of the oxide film. For 99+% pure Ni with oxide thickness ~2.7 μm, the impedance spectra showed a transition from the diffusional impedance for $S_2O_7^{2-}$ in the salt film to an active reaction impedance once the Ni coupon was cathodically polarized from its open-circuit potential into a regime of nickel sulfide stability. The same active reaction impedance was observed for 99+% pure Ni with oxide thickness ~0.8 μm, which suffered from active hot corrosion almost immediately after exposure to the salt film. This active reaction impedance was explained by a model for a preceding EC reaction (oxidation of Ni) coupled with a chemical reaction (basic dissolution of NiO).

For the hot corrosion of metals by fused salts of strong acids, Goebel, Pettit and Goward[11] suggested that the strong acidic oxides MoO_3, WO_3 or V_2O_5 would complex with oxide ions, and thereby, reduce the sulfate solvent basicity, thus increasing the acidic dissolution of the protective oxide. The previously described solubility studies for CeO_2 in fused Na_2SO_4-$NaVO_3$ salt solutions[31,64] provided an important revision to that mechanism. Indeed, in solutions with salts of strong acids, the vanadate, molybdate or tungstate anions are the dominant acidic solutes which complex with oxide ions. But in such salt solutions, all oxides exhibit significantly higher acidic solubilities compared to those in a pure sulfate melt. Therefore, for solutions with strong acidic solutes, the important effect is not a large shift into an acidic regime (on the contrary, the melt becomes more basic), but rather a large rise in oxide solubility. A negative gradient in the concentration for the strong acidic solute can be expected to exist in the salt film as the evaporation of these oxides would occur at the salt/gas interface. Therefore, the "negative solubility gradient" criterion for the solute of the protective oxide scale would be satisfied.

Fryburg, Kohl, Stearns, and Fiedler[65] conducted a detailed study of the initiation of hot corrosion on two preoxidized Al_2O_3-forming Ni-base superalloys, B-1900 and NASA-TRW VIA, which have low Cr (8% and 6%) and high Al (6% and 5.4%) contents. The experiments were performed at 1,173 K in pure oxygen with 3 mg/cm² Na_2SO_4 salt deposit. After an induction period of little corrosion, a local basic fluxing attack of the Cr_2O_3/Al_2O_3 scale spread to cover the alloy surface and generate catastrophic linear kinetics. In the initiation stage, a decrease in sulfate ions correlated to an increase in water-soluble Cr and Al solutes. During the catastrophic attack of B-1900, the sulfate ions reacted to release SO_2 and form sulfides in the alloy, and the salt was converted almost entirely to Na_2MoO_4 as a reaction product from Mo in the alloy. By a sulfate mass balance, the basic fluxing of Al_2O_3, Cr_2O_3, and MoO_3 was demonstrated quantitatively to cause the initiation of rapid corrosion. The AlO_2^- solute precipitated as nonprotective Al_2O_3 in the salt film. During the catastrophic stage, Al_2O_3 and Cr_2O_3 were dissolved by acidic fluxing to form MoO_4^{2-} ions. These experiments provided indisputable evidence for the significance of fluxing reactions.

Later, Fryburg et al.[66] conducted a similar study of the hot corrosion on the preoxidized Cr_2O_3-TiO_2-forming alloy IN 738 at 1,248 K in oxygen. During a long 55-h induction period, first Cr_2O_3 and then TiO_2 were dissolved as basic solutes in Na_2SO_4, with an associated release of SO_2 until all of the Na_2SO_4 was consumed. Thereafter, the liquid $Na_2(MoO_4,WO_4)$ formed by the oxidation of Mo and W served as a flux for the cyclic acidic dissolution of Cr_2O_3 and Al_2O_3 to result in catastrophic kinetics.

In summary, upon generalizing the observations and mechanisms for Type I hot corrosion, the Goebel-Pettit model that the salt basicity can be increased by sulfide formation is certainly valid, and the "negative solubility gradient"[60] has proved to be a useful criterion for sustained hot corrosion. As noted by Shores,[61] this criterion can be readily applied to alloy hot corrosion, whereby a composition gradient of one soluble component in the salt film can set up a negative solubility gradient for another. In the application of the Rapp-Goto criterion to the hot corrosion of transition metals, such as iron and cobalt, particular attention should be paid to the dependence of oxide solubility upon both melt basicity and oxygen activity.

Type II Hot Corrosion

This "low-temperature" hot corrosion (LTHC) occurs well below the melting point of pure Na_2SO_4, 1,157 K. From the LTHC studies, the reaction product morphology is characterized by a non-uniform attack in the form of pits, with only little sulfide formation close to the alloy/scale interface and little depletion of Cr or Al in the alloy substrate. Luthra and Shores[67] conducted experiments on Co-30Cr and Ni-30Cr alloys coated with Na_2SO_4 in $O_2/SO_2/SO_3$ gas environments. A maximum corrosion rate for Co-30Cr was found at 923–973 K with about 90% $CoSO_4$ in a binary $CoSO_4$-Na_2SO_4 liquid phase in an O_2-0.15%(SO_2+SO_3) gas. The maximum kinetics for Ni-30Cr occurred at 973–1,023 K with the formation of a $NiSO_4$-Na_2SO_4 melt of about 45% $NiSO_4$ in an O_2-1.0%(SO_2+SO_3) gas. Assuming that the two binary sulfate systems are regular solutions of molecular species, they calculated the critical partial pressures of SO_3 for the formation of the liquid phases. Misra et al.[28] analyzed the same binary sulfate systems using a regular solution model with Temkin random mixing of ionic species. These calculated values of P_{SO_3} required to support rapid attack agree well with those found experimentally. Thus, acidic fluxing of NiO and CoO occurred at these low temperatures because a liquid phase was stabilized for the corrosion products of Ni and Co by the SO_3/O_2 environment.

In later papers,[68–70] Luthra reported the LTHC behavior for a number of Co-Cr, Co-Al, and Co-Cr-Al alloys. After a low-melting $CoSO_4$-Na_2SO_4 liquid phase was formed, the acidic dissolution of CoO at the oxide/salt interface supported the precipitation of either Co_3O_4 or $CoSO_4$ near the salt/gas interface. The negative solubility gradient was maintained by gradients in the basicity and oxygen activity in the salt film. For sufficient acidic cobalt-solute ions in the salt film, countertransport of Co^{2+}/Co^{3+} ions carried the reduction reaction to the salt/gas interface. In this case, the dissolution/precipitation of cobalt compounds prevents the formation of a protective scale of Cr_2O_3 or Al_2O_3. This important contribution by Luthra was emphasized in a study of Type II hot corrosion of Co-Cr-Al alloys.[70] The resistance of both binary Co-Cr and Co-Al alloys increased with increasing Cr or Al content, respectively. However, the addition of either Cr to a Co-Al alloy or Al to a Co-Cr alloy was deleterious because they disrupt the formation of an $Al_2O_3/CoAl_2O_4$ or $Cr_2O_3/CoCr_2O_4$ protective film, which is needed to prevent the exposure and sulfation of cobalt. Consistent with this model, Luthra and Wood[71] have shown that binary Co-Cr coatings with more than 37.5% Cr and a small reactive element addition provide excellent LTHC resistance.

The hot corrosion behavior of pure iron, and various Fe-Cr and Fe-Al alloys was studied by Zhang, Shih et al.[72–75] in SO_3-containing gas atmospheres at 923–1,023 K for a pure Na_2SO_4 salt deposit, and at 833–1,023 K for a Na_2SO_4-K_2SO_4 salt deposit. A low-melting liquid phase of $Fe_2(SO_4)_3$-Na_2SO_4 or $Fe_2(SO_4)_3$-Na_2SO_4-K_2SO_4 was formed. A maximum corrosion rate was observed for the Fe-Cr alloys at about 973 K and for the Fe-Al

alloys at about 923 K. These results were interpreted by the dissolution/precipitation mechanism: Fe^{3+} ions were reduced at the scale/salt interface to form Fe^{2+} ions, and the countermigration of Fe^{3+}/Fe^{2+} ions in the salt film carried the O_2 reduction reaction to the salt/gas interface. Thus, a negative solubility gradient across the salt film was satisfied for acidic iron solutes. Consistent with the work of Luthra and Wood,[71] a diffusion coating with about 50% Cr at its outermost surface provided excellent protection for iron.[76]

CONCLUDING REMARKS

The important fundamental studies summarized in this paper clearly indicate that considerable progress has been made in understanding the hot corrosion of materials. At the same time, materials and protective coatings resistant to hot corrosion have been developed. The ultimate establishment of a generalized hot corrosion mechanism may not ever succeed; however, a quantitative knowledge of oxide solubilities and EC reduction reactions is very important in clarifying hot corrosion phenomena. From the Rapp-Goto criterion, the formation of a protective oxide scale involving a minimum number of components is preferred. For example, a scale consisting exclusively of Cr_2O_3 or of SiO_2 exhibits excellent resistance in acidic sulfates because neither a negative solubility gradient nor a synergistic fluxing is expected. The presence of strong acidic components in the salt film introduce a significant increase in the acidic solubilities for all oxides, and therewith accelerated hot corrosion.

ACKNOWLEDGEMENTS

The research performed at the Ohio State University was sponsored by the National Science Foundation, Electric Power Research Institute, General Electric Company, and the Office of Naval Research, project N14-92-J-1229, A.J. Sedriks, project monitor.

References

1. W.T. Reid, R.C. Corey, and B.J. Cross, *Trans. ASME*, 67 (1945), p. 279.
2. F.J. Wall and S.T. Michael, *ASTM Spec. Tech. Publ. STP 421* (1967), p. 223.
3. E. Erdos, *Deposition and Corrosion in Gas Turbines*, ed. A.B. Hart and A.J.B. Cutler (London: Applied Science Publishers, 1973), p. 115.
4. K.J. Kohl et al., *J. Electrochem. Soc.*, 126 (1979), p. 1054.
5. K.L. Luthra and H.S. Spacil, *J. Electrochem. Soc.*, 129 (1982), p. 649.
6. E.L. Simons, G.V. Browning, and H.A. Liebhafsky, *Corrosion*, 11 (1955), p. 505.
7. A.U. Seybolt, *Trans. AIME*, 242 (1968), p. 1955.
8. N.S. Bornstein and M.A. DeCrescente, *Trans. AIME*, 245 (1969), p. 583.
9. N.S. Bornstein and M.A. DeCrescente, *Met. Trans.*, 2 (1971), p. 2875.
10. J.A. Goebel and F.S. Pettit, *Met. Trans.*, 1 (1970), p. 1943.
11. J.A. Goebel, F.S. Pettit, and G.W. Goward, *Met. Trans.*, 4 (1973), p. 261.
12. J. Stringer, *Annual Review of Materials Sci.*, 7, ed. R.A. Huggins (Palo Alto, CA: Annual Review Inc., 1977), p. 449.
13. J. Stringer, *Materials Sci. Techn.*, 3 (1987), p. 482.
14. F.S. Pettit and C.S. Giggins, "Hot Corrosion," *Superalloys II*, ed. C.T. Sims, N.S. Stoloff, and W.C. Hagel (New York: Wiley Publ., 1987), p. 327.
15. R.A. Rapp, *Corrosion*, 42 (1986), p. 568.
16. R.A. Rapp, "Hot Corrosion of Materials," *Selected Topics in High Temperature Chemistry*, ed. O. Johannesen and A.G. Andersen (Amsterdam: Elsevier, 1989), p. 291.
17. C.O. Park and R.A. Rapp, *J. Electrochem. Soc.*, 133 (1986), p. 1636.
18. D. Inman and D.M. Wrench, *Brit. Corros. J.*, 1 (1966), p. 246.
19. D.A. Shores and R.C. John, *J. Appl. Electrochem.*, 10 (1980), p. 275.
20. P.P. Leblanc and R.A. Rapp, *J. Electrochem. Soc.*, 139 (1992), p. L31.
21. P.P. Leblanc and R.A. Rapp, *J. Electrochem. Soc.*, 140 (1993), p. L41.
22. D.K. Gupta and R.A. Rapp, *J. Electrochem. Soc.*, 127 (1980), p. 2194 and 2656.
23. Y.S. Zhang and R.A. Rapp, *J. Electrochem. Soc.*, 132 (1985), p. 734 and 2498.
24. Y.S. Zhang, *J. Electrochem. Soc.*, 133 (1986), p. 655.
25. P.D. Jose, D.K. Gupta, and R.A. Rapp, *J. Electrochem. Soc.*, 132 (1985), p. 735.
26. D.Z. Shi and R.A. Rapp, *J. Electrochem. Soc.*, 133 (1986), p. 849.
27. M.L. Deanhardt and K.H. Stern, *J. Electrochem. Soc.*, 128 (1981), p. 2577.
28. A.K. Misra, D.P. Whittle, and W.L. Worrell, *J. Electrochem. Soc.*, 129 (1982), p. 1840.
29. M.L. Deanhardt and K.H. Stern, *J. Electrochem. Soc.*, 129 (1982), p. 2228.
30. N.S. Jacobson and J.L. Smialek, *J. Amer. Ceram. Soc.*, 68 (1985), p. 432.
31. N.S. Jacobson, *J. Amer. Ceram. Soc.*, 76 (1993), p. 3.
32. Y.S. Hwang and R.A. Rapp, *J. Electrochem. Soc.*, 137 (1990), p. 1276.
33. Y.S. Zhang and R.A. Rapp, *Corrosion*, 43 (1987), p. 348.
34. Y.S. Hwang and R.A. Rapp, *Corrosion*, 45 (1989), p. 933.
35. R.A. Rapp and Y.S. Zhang, "Electrochemical Studies of Hot Corrosion of Materials," *Proc. Intern. Corr. Conf.* (Merida, Mexico: 1993)
36. R.L. Jones, D.B. Nordman, and S.T. Gadomski, *Met. Trans.*, 16A (1985), p. 303.
37. R.L. Jones, S.R. Jones, and C.E. Williams, *J. Electrochem. Soc.*, 132 (1985), p. 1499.
38. R.L. Jones, C.E. Williams, and S.R. Jones, *J. Electrochem. Soc.*, 133 (1986), p. 227.
39. R.L. Jones and D. Mess, *J. Amer. Ceram. Soc.*, 75 (1992), p. 1818.
40. R.L. Jones, *High Temp. Tech.*, 6 (1988), p. 187.
41. M. Seiersten and P. Kofstad, *Mater. Sci. Tech.*, 3 (1987), p. 576.
42. A.S. Nagelberg, *J. Electrochem. Soc.*, 132 (1985), p. 2502.
43. F. Mansfeld and J.V. Kenkel, *Corr. Sci.*, 16 (1976), p. 111.
44. F. Mansfeld and J.V. Kenkel, *Corrosion*, 33 (1977), p. 238.
45. R. Andresen, *J. Electrochem. Soc.*, 126 (1979), p. 328.
46. D.A. Shores and W.C. Fang, *J. Electrochem. Soc.*, 128 (1981), p. 346.
47. W.C. Fang and R.A. Rapp, *J. Electrochem. Soc.*, 130 (1983), p. 2335.
48. H. Numata, A. Nishikata, and S. Haruyama, *Proc. JIMIS-3, Trans. Japan Inst. Suppl.* (1983), p. 303.
49. X. Zheng and R.A. Rapp, *J. Electrochem. Soc.*, 140 (1993), p. 2857.
50. H. Numata and S. Haruyama, *Corrosion*, 44 (1988), p. 7249.
51. J. Kupper and R.A. Rapp, *Werkstoffe und Korrosion*, 38 (1987), p. 674.
52. J.C. Nava, D.Z. Shi, and R.A. Rapp, "Electrochemical Reactions of $NaVO_3$ and Na_2CO_4 Solutes in Na_2SO_4," *High Temperature Materials Chemistry IV* (Pennington, NJ: Electrochem. Soc., 1987), p. 1.
53. D.Z. Shi and R.A. Rapp, *Werkstoffe und Korrosion*, 41 (1990), p. 215.
54. D.A. Shores, *Corrosion*, 31 (1975), p. 434.
55. A. Rahmel, M. Schmidt, and M. Schorr, *Oxid. Metals*, 18 (1982), p. 195.
56. W.T. Wu, A. Rahmel, *Oxid. Metals*, 19 (1983), p. 201.
57. W.T. Wu, A. Rahmel, and M. Schorr, *Oxid. Metals*, 22 (1984), p. 59.
58. W.T. Wu, J. Zhang, and Y. Niu, *Proc. 11th Intern. Cong. Mater. Corr.* (Florence, Italy, April 2–6, 1990), p. 1475.
59. Y. Niu, J. Zhang, and W.T. Wu, *High Temperature Corrosion and Protection*, ed. H. Guan, W.T. Wu , J. Shen, and T. Li (Shenyang, China: Liaoning Sci. Techn. Publ. House, 1990), p. 201.
60. R.A. Rapp and K.S. Goto, "Hot Corrosion of Metals by Molten Salts," *Molten Salts I*, ed. J. Braunstein and J.R. Selman (Pennington, NJ: Electrochem. Soc., 1981), p. 159.
61. D.A. Shores, "New Perspective on Hot Corrosion Mechanisms," *High Temperature Corrosion, NACE-6*, ed. R.A. Rapp (Houston, TX: NACE, 1983), p. 493.
62. N. Otsuka and R.A. Rapp, *J. Electrochem. Soc.*, 137 (1990), p. 46.
63. Y.M. Wu and R.A. Rapp, *J. Electrochem. Soc.*, 138 (1991), p. 2683.
64. Y.S. Zhang and R.A. Rapp, "Solubility of CeO_2 in Molten Na_2SO_4-10 mol.% $NaVO_3$ salt solution at 900°C" (Paper to be presented at 9th Intern. Symp. Molten Salts, San Francisco, 22–27 May 1994).
65. G.C. Fryburg et al., *J. Electrochem. Soc.*, 129 (1982), p. 571.
66. G.C. Fryburg, F.J. Kohl, and C.A. Stearns, *J. Electrochem. Soc.*, 131 (1984), p. 2985.
67. K.L. Luthra and D.A. Shores, *J. Electrochem. Soc.*, 127 (1980), p. 2202.
68. K.L. Luthra, *High Temperature Corrosion, NACE-6*, ed. R.A. Rapp (Houston, TX: NACE, 1983), p. 507.
69. K.L. Luthra, *Met. Trans.*, 13A (1982), pp. 1647, 1843, and 1853.
70. K.L. Luthra, *J. Electrochem. Soc.*, 132 (1985), p. 1293.
71. K.L. Luthra and J.H. Wood, *Thin Solid Films*, 119 (1984), p. 271.
72. Y.S. Zhang, L.Q. Shi, and S.T. Shih, *J. Chin. Soc. Corr. Protec.*, 12 (1992), p. 189.
73. Y.S. Zhang, X.M. Li, L.Q. Shi, and S.T. Shih, *J. Chin. Soc. Corr. Protec.*, 11 (1991), p. 17.
74. L.Q. Shi, Y.S. Zhang, and S.T. Shih, *Corr. Sci.*, 33 (1992), p. 1427.
75. L.Q. Shi, Y.S. Zhang, and S.T. Shih, *Oxid. Metals*, 38 (1992), p. 385.
76. Y.S. Zhang, X.M. Li, T.L. Cao, and S.T. Shih, *Corr. Sci. Protec. Tech.*, 4 (1992), p. 9.

ABOUT THE AUTHORS

Robert A. Rapp earned his Ph.D. in metallurgical engineering at Carnegie-Mellon University in 1959. He is currently M.G. Fontana Professor at the Ohio State University. Dr. Rapp is also a fellow of TMS.

Yun-Shu Zhang earned his Ph.D. in metallurgical engineering at Shanghai Institute of Metallurgy, Chinese Academy of Sciences, China in 1982. He is currently a visiting scholar at The Ohio State University.

For more information, contact Robert A. Rapp, the Ohio State University, Department of Materials Science and Engineering, Columbus, Ohio 43210; telephone (614) 292-6178; fax (614) 292-1537; e-mail: rappbob@kcg.eng.ohio-state.edu.